Pergamon

SCIENCE DIRECT®

Tetrahedron 59 (2003) 5307–5315

TETRAHEDRON

New antimitotic bicyclic peptides, celogentins D–H, and J, from the seeds of *Celosia argentea*

Hayato Suzuki,[a] Hiroshi Morita,[a] Shigeo Iwasaki[b] and Jun'ichi Kobayashi[a,*]

[a]*Graduate School of Pharmaceutical Sciences, Hokkaido University, Sapporo 060-0812, Japan*
[b]*Kitasato Institute for Life Science, Kitasato University, Tokyo 108-8642, Japan*

Received 21 April 2003; revised 9 May 2003; accepted 12 May 2003

Abstract—Six new bicyclic peptides, celogentins D–H (**1**–**5**) and J (**6**) have been isolated from the seeds of *Celosia argentea*, and the structures including its absolute stereochemistry were determined by using extensive NMR methods and chemical means. Celogentins E–H (**2**–**5**) and J (**6**) showed potent inhibition of tubulin polymerization, while the inhibitory activity of celogentin D (**1**) was modest. Structure–activity relationship study indicates that ring size of the bicyclic ring system including unusual β^s-Leu, Trp, and His residues would be important for their biological activity.

Tubulin is the main structural component of microtubules, which play important roles in mitosis, cell signaling and motility in eucaryotes, and interacts with a wide range of natural compounds.[1] Among them, two representative antimitotic drugs, paclitaxel, which induces microtubule bundling, and vinblastine, which induces microtubule disassembly, bind to different sites of tubulin and show opposite effects in vitro.[1] The antimitotic agents interfering with the natural dynamics of tubulin polymerization and depolymerization have potential applications in drug development and have received a considerable amount of attention.[2]

Previous studies have shown that three new bicyclic peptides, celogentins A–C (**7**–**9**),[3] and moroidin (**10**),[4] from the seeds of *Celosia argentea* (Amaranthaceae) remarkably inhibited the tubulin polymerization. During our continuous search for antimitotic compounds from *C. argentea*, we isolated six new bicyclic peptides, celogentins D–H (**1**–**5**) and J (**6**), which showed inhibition of the tubulin polymerization. In this paper we describe the isolation, structure elucidation, and antimitotic activity of **1**–**6**.

1. Structure elucidation

The seeds of *C. argentea* were extracted with MeOH, and the MeOH extract was in turn partitioned with hexane, EtOAc, and *n*-BuOH. *n*-BuOH-soluble materials were subjected to a Diaion HP-20 column ($MeOH/H_2O$, 0:1→1:0), in which each fraction eluted with 60, 80, and 100% MeOH, respectively, was purified by an amino silica gel column ($CHCl_3/MeOH/H_2O$, 7:3:0.5→6:4:1) followed by C_{18} HPLC (23–34% CH_3CN/0.1% CF_3CO_2H) to afford celogentins D (**1**, 0.00004% yield), E (**2**, 0.0008%), F (**3**,

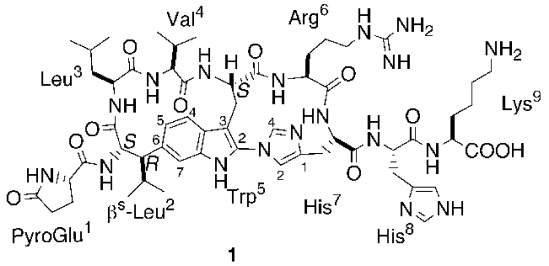

1

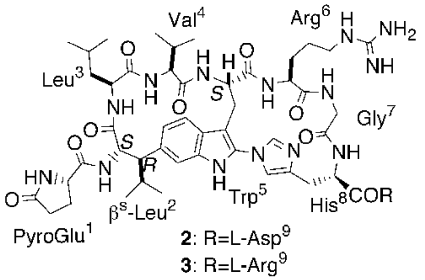

2: R=L-Asp[9]
3: R=L-Arg[9]

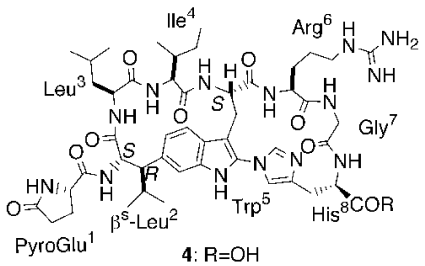

4: R=OH
5: R=L-Asp[9]
6: R=L-Arg[9]

Keywords: peptides; *Celosia argentea*; tubulin polymerization.

* Corresponding author. Tel.: +81-117064985; fax: +81-117064989; e-mail: jkobay@pharm.hokudai.ac.jp

0040–4020/03/$ - see front matter
doi:10.1016/S0040-4020(03)00762-2

Table 1. ^{1}H NMR data {δ_H [int. mult, J (Hz)]} of Celogentins D–H (**1**–**5**) and J (**6**) in DMSO-d_6

	1[a]	**2**[b]	**3**[b]	**4**[b]	**5**[b]	**6**[b]
PyroGlu[1]						
α	4.15 (m)	4.17 (m)	4.11 (m)	4.08 (dd, 3.5, 9.3)	4.11 (m)	4.11 (m)
β	1.73, 2.25 (m)	1.73, 2.27 (m)	2.25, 1.73 (m)	1.69, 2.21 (m)	1.71, 2.24 (m)	1.72, 2.25 (m)
γ	2.11(m)	2.11 (m)	2.09 (m)	2.05 (m)	2.09 (m)	2.09 (m)
NH	7.81 (s)	7.85 (s)	7.82 (s)	7.79 (s)	7.82 (s)	7.82 (s)
β[s]-Leu[2]						
α	5.00 (t, 10.2)	4.88 (t, 10.0)	4.85 (m)	4.82 (t, 10.5)	4.86 (1H, m)	4.85 (m)
β	2.98 (dd, 3.3, 11.6)	3.08 (dd, 3.6, 11.9)	3.14 (dd, 3.3, 11.6)	3.01 (dd, 3.6, 11.0)	3.04 (dd, 3.1, 11.9)	3.04 (m)
γ	2.13 (1H, m)	2.17 (1H, m)	2.14 (m)	2.13 (m)	2.13 (m)	2.14 (m)
δ	0.84 (d, 6.3)	0.79 (m)	0.76 (m)	0.73 (m)	0.75 (m)	0.75 (m)
	0.86 (d, 5.2)	0.87 (m)	0.84 (d, 6.6)	0.80 (m)	0.84 (d, 7.0)	0.84 (d, 6.3)
NH	8.50 (d, 8.6)	8.49 (d, 8.8)	8.47 (m)	8.43 (d, 8.8)	8.45 (d, 9.8)	8.46 (m)
Leu[3]						
α	4.13 (m)	4.02 (dt, 4.1, 10.6)	3.99 (m)	3.95 (dt, 3.7, 9.2)	3.98 (dt, 3.6, 10.1)	3.98 (dt, 10.2, 4.3)
β	1.33, 1.42 (m)	1.21, 1.49 (m)	1.20, 1.46 (m)	1.16, 1.40 (m)	1.18, 1.43 (m)	1.19, 1.43 (m)
γ	1.40 (m)	1.50 (m)	1.43 (m)	1.39 (m)	1.41 (m)	1.41 (m)
δ	0.73 (d, 5.5)	0.72 (d, 6.4)	0.69 (d, 5.9)	0.65 (d, 6.3)	0.69 (d, 6.0)	0.69 (d, 6.0)
	0.79 (d, 5.7)	0.81 (d, 6.5)	0.78 (m)	0.73 (m)	0.78 (d, 5.9)	0.77 (m)
NH	8.57 (d, 10.2)	8.35 (d, 9.3)	8.33 (d, 9.2)	8.30 (d, 9.7)	8.33 (d, 9.6)	8.33 (d, 9.6)
Val[4]						
α	4.11 (dd, 4.6, 8.8)	3.67 (t, 7.3)	3.68 (m)			
β	2.41 (m)	1.84 (m)	1.82 (m)			
γ	0.94 (d, 6.8)	0.78 (m)	0.76 (m)			
	1.10 (d, 6.9)	0.83 (m)	0.76 (m)			
NH	6.54 (d, 8.7)	6.97 (d, 7.7)	6.93 (d, 6,6)			
Ile[4]						
α				3.74 (t, 7.4)	3.71 (m)	3.73 (m)
β				1.61 (m)	1.60 (m)	1.62 (m)
γ1				0.73 (m)	0.74 (m)	0.75 (m)
γ2				0.97, 1.30 (m)	0.94, 1.30 (m)	0.95 (m)
δ				0.81 (m)	0.76 (m)	0.75 (m)
NH				6.87 (m)	6.93 (d, 7.5)	6.92 (d, 8.2)
Trp[5]						
α	4.85 (m)	5.52 (br s)	5.46 (m)	5.37 (m)	5.48 (br s)	5.46 (m)
β	2.86 (d, 14.3)	2.64 (m)	2.66 (m)	2.63 (m)	2.62 (m)	2.66 (m)
	3.24 (m)	3.37 (m)	3.34 (m)	3.31 (m)	3.32 (m)	3.32 (m)
NH1	11.41 (s)	11.50 (s)	11.44 (s)	11.56 (s)	11.48 (s)	11.44 (s)
H4	7.37 (d, 8.3)	7.57 (d, 8.5)	7.53 (d, 8.7)	7.49 (d, 8.7)	7.54 (d, 9.2)	7.53 (d, 8.7)
H5	7.14 (d, 8.0)	7.00 (d, 8.1)	6.98 (d, 8.6)	6.98 (d, 9.1)	6.98 (d, 8.8)	6.98 (d, 8.6)
H7	6.91 (s)	6.91 (s)	6.87 (s)	6.87 (s)	6.89 (s)	6.87 (s)
NH	6.35 (d, 8.0)	8.01 (d, 8.8)	7.90 (d, 8.8)	7.67 (d, 6.3)	7.95 (d, 9.8)	7.87 (d, 9.2)
Arg[6]						
α	4.36 (m)	4.13 (m)	4.12 (m)	4.13 (q, 6.8)	4.10 (m)	4.12 (m)
β	1.38, 1.51 (m)	1.59, 1.74 (m)	1.56, 1.73 (m)	1.60, 1.69 (m)	1.63, 1.69 (m)	1.54, 1.70 (m)
γ	1.38 (m)	1.58 (m)	1.56 (m)	1.49 (m)	1.57 (m)	1.56 (m)
δ	3.07 (m)	3.18 (d, 7.0)	3.14 (m)	3.09 (m)	3.14 (m)	3.13 (d, 7.0)
ε(NH)	7.59 (br s)	7.71 (m)	7.76 (m)	7.77 (t, 5.8)	7.72 (br s)	7.74 (m)
NH	8.21 (d, 8.0)	8.73 (d, 5.4)	8.66 (d, 6.8)	8.51 (d, 6.3)	8.68 (d, 6.2)	8.65 (m)
His[7]						
α	4.62 (m)					
β	2.54 (m)					
	3.04 (m)					
H2	6.97 (br s)					
H4	7.64 (br s)					
Gly[7]						
α		3.73 (br s)	3.66, 3.72 (m)	3.62, 3.69 (m)	3.68, 3.72 (m)	3.69, 3.72 (m)
NH		7.14 (br s)	7.26 (m)	7.44 (d, 9.5)	7.13 (br s)	7.28 (m)
His[8]						
α	4.66 (t, 6.2)	4.92 (t, 9.2)	4.84 (m)	4.70 (t, 9.9)	4.88 (m)	4.84 (m)
β	3.00 (m)	2.82 (m)	2.80 (m)	2.90 (br t, 12.3)	2.80 (br s)	2.79 (m)
	3.13 (m)	3.14 (m)	3.04 (m)	3.16 (m)	3.09 (m)	3.04 (m)
H2	7.21 (br s)	7.37 (m)	7.21 (m)	7.44 (m)	7.35 (br s)	7.32 (m)
H4	8.64 (br s)	8.03 (m)	7.77 (m)	8.30 (m)	8.02 (br s)	7.75 (m)
NH	8.16 (d, 7.7)	8.60 (m)	8.47 (m)	8.47 (d, 6.7)	8.58 (d, 9.6)	8.46 (m)

Table 1 (*continued*)

	1[a]	**2**[b]	**3**[b]	**4**[b]	**5**[b]	**6**[b]
Lys[9]						
α	4.19 (m)					
β	1.63, 1.77 (m)					
γ	1.38 (m)					
δ	1.55 (m)					
ε	2.79 (t, 6.8)					
NH	8.22 (m)					
Asp[9]						
α		4.59 (q, 7.3)			4.56 (q, 6.5)	
β		2.53 (dd, 7.2, 15.5)			2.51 (dd, 7.0, 15.3)	
		2.61 (dd, 5.3, 15.5)			2.57 (dd, 5.4, 15.5)	
NH		8.47 (d, 7.7)			8.42 (d, 7.7)	
Arg[9]						
α			4.23 (q, 7.6)			4.23 (q, 6.4)
β			1.65, 1.78 (m)			1.64, 1.78 (m)
γ			1.56 (m)			1.56 (m)
δ			3.14 (m)			3.13 (m)
ε (NH)			7.76 (m)			7.74 (m)
NH			8.42 (m)			8.42 (m)

[a] 315 K.
[b] 310 K.

0.001%), G (**4**, 0.0007%), H (**5**, 0.00004%), and J (**6**, 0.00003%) as colorless solids together with celogentins A–C (**7**–**9**)[3] and moroidin (**10**).[5]

FABMS data of celogentin D (**1**) {$[\alpha]_D^{24}=-33°$ (*c* 0.4, 50% MeOH)} showed the pseudomolecular ion at *m/z* 1196 $(M+H)^+$, and the molecular formula, $C_{57}H_{82}N_{18}O_{11}$, was established by HRFABMS [*m/z* 1195.6480, $(M+H)^+$, Δ −1.0 mmu]. IR absorptions implied the presence of amide carbonyl group (1660 cm^{-1}), while the UV absorption at 283 nm indicated the presence of aromatic chromophore.

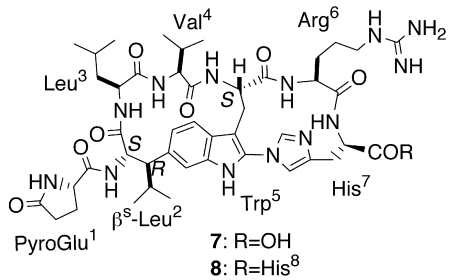

7: R=OH
8: R=His[8]

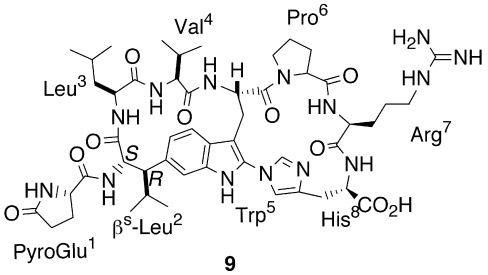

9

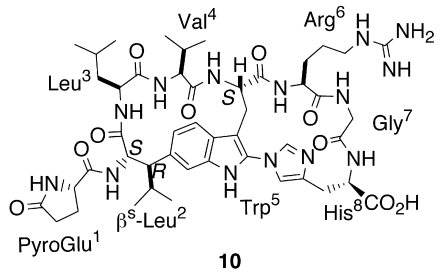

10

Standard amino acid analysis of the hydrolysates of **1** showed the presence of 1 mol of glutamic acid (Glu), leucine (Leu), valine (Val), arginine (Arg), and lysine (Lys), and 2 mol of histidine (His). The ^1H NMR (Table 1) spectrum of **1** in DMSO-d_6 showed nine proton resonances (δ 4.11–5.00), which were indicative of α-protons of amino acid residues. The presence of 6 methyl groups, 13 methylenes, 13 methines, and 7 olefins was indicated by the ^{13}C NMR (Table 2) spectrum. The unusual amino acids, β-substituted Leu (β^s-Leu) and 2,6-substituted Trp (Trp), which have been previously observed for celogentins A–C (**7**–**9**),[3] were revealed by analysis of the ^1H and ^{13}C NMR data (Tables 1 and 2, respectively) aided by ^1H–^1H COSY, HOHAHA, HMQC, and HMBC experiments. These data combined with observation of ten carbonyl signals (δ 169.02–177.23) including a PyroGlu residue suggested that **1** was a nonapeptide.

The cyclic peptide nature and sequence (PyroGlu[1]-β^s-Leu[2]-Leu[3]-Val[4]-Trp[5]-Arg[6]-His[7]-His[8]-Lys[9]) of celogentin D (**1**) were elucidated by detailed analysis of NOESY correlations as shown in Figure 1. The connection between C-2 of Trp[5] and N-3 of His[7] was suggested by NOESY correlations of H-2 and H-4 of His[7]/NH-1 of Trp[5]. The connection between Cβ of β^s-Leu[2] and C-6 of Trp[5] was deduced from NOESY correlations of H-5 of Trp/Hα and Hγ of β^s-Leu and H-7 of Trp/Hβ of β^s-Leu and ^3J coupling (11.0 Hz) between Hα and Hβ of β^s-Leu as shown in computer-generated 3D drawing (Fig. 2). Thus, the whole sequence of celogentin D was assigned as **1**.

The absolute configurations of the PyroGlu[1], Leu[3], Val[4], Arg[6], His[7], His[8], and Lys[9] residues in celogentin D (**1**) were assigned as all L-configurations by chiral HPLC analysis of the hydrolysates of **1**. The Trp[5] residue was transformed into

Table 2. ^{13}C NMR data (δ_C) of Celogentins D–H (**1**–**5**) and J (**6**) in DMSO-d_6

		1[a]	**2**[b]	**3**[b]	**4**[b]	**5**[b]	**6**[b]
PyroGlu[1]	α	54.87	54.81	54.58	55.03	55.06	54.85
	β	25.29	25.45	24.91	25.36	25.38	25.18
	γ	28.74	28.98	28.40	28.89	28.90	28.64
	δ	177.23	177.30	177.12	177.35	177.38	177.38
	C=O	172.27	172.51	171.64	172.09	172.06	171.86
β[s]-Leu[2]	α	54.80	54.72	54.23	54.75	54.70	54.52
	β	52.55	51.40	50.93	51.53	51.36	51.39
	γ	26.77	26.70	26.12	26.64	26.59	26.40
	δ	17.33	17.34	16.62	17.12	17.10	18.39
		23.00	22.54	21.20	22.90	21.69	22.73
	C=O	169.80	169.33	170.45	171.45	171.40	170.77
Leu[3]	α	51.09	52.00	51.52	51.89	51.99	51.75
	β	43.49	41.80	41.32	41.94	41.71	41.61
	γ	23.45	23.84	23.34	23.78	24.27	24.12
	δ	20.63	21.28	20.33	20.83	20.84	20.64
		21.81	22.56	22.46	21.91	22.93	21.49
	C=O	173.04	171.46	168.91	171.98	170.40	169.19
Val[4]	α	58.61	57.55	57.05			
	β	29.28	31.11	30.33			
	γ	16.54	18.51	17.83			
		18.90	22.66	21.44			
	C=O	169.23	168.17	168.75			
Ile[4]	α				56.71	56.51	56.35
	β				36.89	37.03	36.76
	γ1				14.30	14.19	14.04
	γ2				24.36	23.25	22.73
	δ				11.40	11.43	11.22
	C=O				169.43	169.35	168.92
Trp[5]	α	52.02	48.94	48.56	49.11	48.83	48.89
	β	25.70	27.07	26.56	26.58	27.02	26.40
	C2	119.90	128.53	126.10	127.78	124.97	124.91
	C3	102.74	101.53	100.68	102.46	101.32	102.35
	C4	117.80	119.22	118.65	119.17	119.21	119.17
	C5	119.80	119.36	118.84	119.62	119.39	118.89
	C6	131.85	131.65	131.83	132.72	119.22	130.64
	C7	114.45	113.96	113.45	114.06	113.96	113.71
	C8	132.50	132.67	132.20	131.46	137.35	132.45
	C9	125.60	124.98	124.97	124.97	132.68	125.23
	C=O	169.02	169.21	169.02	169.11	171.17	171.23
Arg[6]	α	51.06	54.18	53.35	53.43	53.96	53.60
	β	29.73	28.17	27.63	28.51	27.94	27.95
	γ	24.80	25.27	24.70	25.00	25.16	24.94
	δ	40.15	40.43	39.75	40.24	40.26	39.97
	ε	156.70	156.80	156.46	156.88	156.81	156.71
	C=O	170.40	171.11	170.40	171.80	172.49	172.83
His[7]	α	52.55					
	β	31.03					
	C1	128.90					
	C2	120.05					
	C4	137.98					
	C=O	170.80					
Gly[7]	α		42.61	42.15	42.58	42.59	42.48
	C=O		168.19	167.71	168.38	168.19	167.98
His[8]	α	51.17	50.38	50.07	51.37	50.37	50.42
	β	27.01	31.95	31.72	29.34	31.73	30.93
	C1	125.70	131.43	130.37	134.28	130.96	131.44
	C2	116.75	117.56	116.35	118.84	117.69	117.05
	C4	134.20	137.40	136.38	137.27	137.33	137.46
	C=O	170.60	170.39	171.05	171.55	171.49	171.31
Lys[9]	α	51.85					
	β	30.25					
	γ	24.27					
	δ	51.85					
	ε	30.25					

Table 2 (*continued*)

		1[a]	**2**[b]	**3**[b]	**4**[b]	**5**[b]	**6**[b]
	C=O	170.90					
Asp[9]	α		48.72			48.85	
	β		36.51			36.34	
	γ		172.49			173.25	
	δ		172.06			174.32	
Arg[9]	α			51.17			51.22
	β			27.44			27.68
	γ			24.91			24.94
	δ			39.75			39.97
	ε			156.46			156.71
	C=O			172.55			173.25

[a] 315 K.
[b] 310 K.

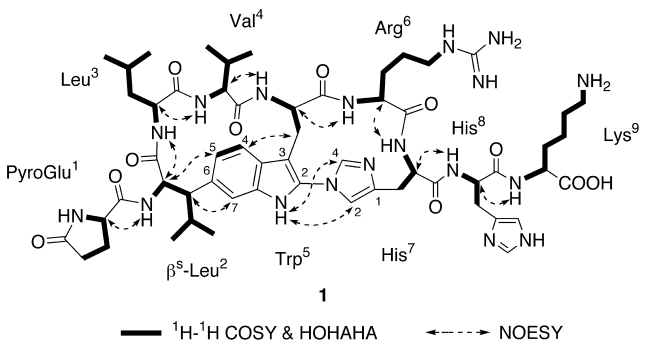

Figure 1. Selected 2D NMR correlations for celogentin D (**1**).

Asp by treatment of **1** with O_3/AcOH and then H_2O_2 followed by acid hydrolysis.[3] Chiral HPLC analysis of the Asp in the degradation products revealed it to be L-form, indicating *S*-configuration at Cα of the Trp[5] residue. Since almost the same NOESY correlations and vicinal coupling around β[s]-Leu[2] residue of **1** as those of moroidin (**10**) were observed, the absolute configurations at Cα and Cβ of the β[s]-Leu[2] residue were elucidated to be *S* and *R*, respectively. Therefore, the structure of celogentin D was concluded to be **1**.

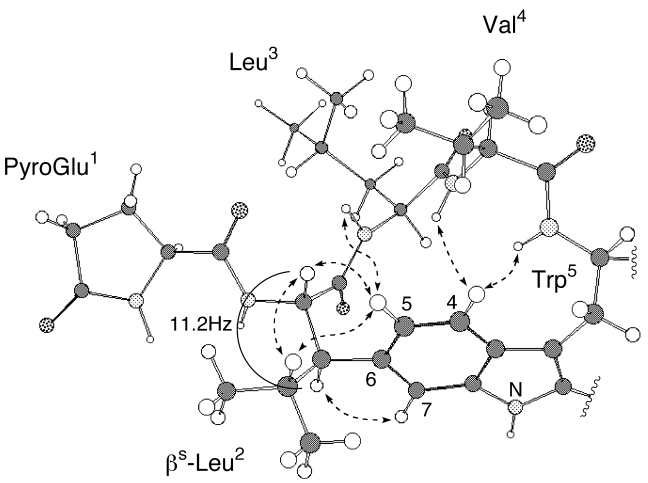

Figure 2. Selected NOESY correlations (dotted arrows) for left hand part of celogentin D (**1**). To clarify the backbone structure, the right-hand part was omitted.

HRFABMS data [*m/z* 1101.5360, $(M)^+$, Δ +0.4 mmu] of celogentin E (**2**) indicated the molecular formula to be $C_{51}H_{71}N_{15}O_{13}$. The IR absorption (1660 cm^{-1}) implied the presence of amide carbonyl functionality. Amino acid analysis of the hydrolysates of **2** showed the presence of 1 mol each of Glu, Leu, Val, Arg, Gly, His, and Asp. The ^1H and ^{13}C NMR (Tables 1 and 2, respectively) spectra of **2** revealed signals due to 10 carbonyl carbons, 12 sp^3 methines, 10 methylenes, and 6 methyl, implying that **2** was also nonapeptide. Detailed analyses of 2D NMR ($^1H-^1H$ COSY, HOHAHA, HMQC, and HMBC) spectra of **2** and comparison of the ^{13}C chemical shifts of the bicyclic part of **2** with those of moroidin (**10**)[5] indicated the presence of the same bicyclic skeleton as that of **10**. The remaining Asp residue was suggested to be connected to His^8 from NOESY correlations of Hα and $H_2β$ of His^8/amide NH of Asp^9.

The absolute configurations of the $PyroGlu^1$, Leu^3, Val^4, Arg^6, His^8, and Asp^9 residues in **2** were assigned as all L-configurations by chiral HPLC analysis of the hydrolysates of **2**. The absolute configurations of the $β^s$-Leu^2 and the Trp^5 residue were elucidated to be the same as those of **1** by the same methods described above. Thus, the structure of celogentin E was determined to be **2**.

HRFABMS data [*m/z* 1143.6180, $(M+H)^+$, Δ +0.4 mmu] of celogentin F (**3**) indicated the molecular formula to be $C_{53}H_{78}N_{18}O_{11}$. The IR absorption (1660 cm^{-1}) implied the presence of amide carbonyl functionality. Amino acid analysis of the hydrolysates of **3** showed the presence of 1 mol each of Glu, Leu, Val, Gly, and His, and 2 mol of Arg. Detailed analyses of 2D NMR spectra of **3** indicated the presence of the same bicyclic skeleton from $PyroGlu^1$ to His^8 as that of **2**. NOESY correlations of Hα and $H_2β$ of His^8/amide NH of Arg^9 indicated that **3** possessed Arg^9 in place of Asp^9 of **2** in the N-terminus. The absolute configuration of each amino acid in **3** was assigned as all L-configurations by chiral HPLC analysis of the hydrolysates of **3**.

HRFABMS data [*m/z* 1001.5340, $(M+H)^+$, Δ +1.8 mmu] of celogentin G (**4**) revealed the molecular formula to be $C_{48}H_{68}N_{14}O_{10}$. Amino acid analysis of the hydrolysates of **4** showed the presence of 1 mol each of Glu, Leu, isoleucine (Ile), Arg, and His. The ^1H and ^{13}C NMR (Tables 1 and 2, respectively) spectra of **4** revealed the presence of nine carbonyl carbons, 12 sp^3 methines, 9 methylenes, and 6 methyls. The structure of **4** was elucidated by 2D NMR ($^1H-^1H$ COSY, HOHAHA, HMQC, and HMBC) data. HMBC and NOESY (Fig. 3) correlations indicated that celogentin G (**4**) possessed Ile in place of Val of moroidin (**10**).[5] The absolute configuration of each amino acid in **4** was assigned as all L-configurations by chiral HPLC analysis of the hydrolysates of **4**. Therefore, the structure of celogentin G was determined to be **4**.

Celogentins H (**5**) and J (**6**) were shown to have the molecular formulae, $C_{52}H_{73}N_{15}O_{13}$ and $C_{54}H_{80}N_{18}O_{11}$, respectively, by HRFABMS data [*m/z* 1115.5570, $(M)^+$, Δ +5.8 mmu for **5**; 1157.6340, $(M+H)^+$, Δ +0.8 mmu for **6**]. Amino acid analysis of the hydrolysates of **5** showed the presence of 1 mol each of Glu, Leu, Ile, Arg, His, and Asp,

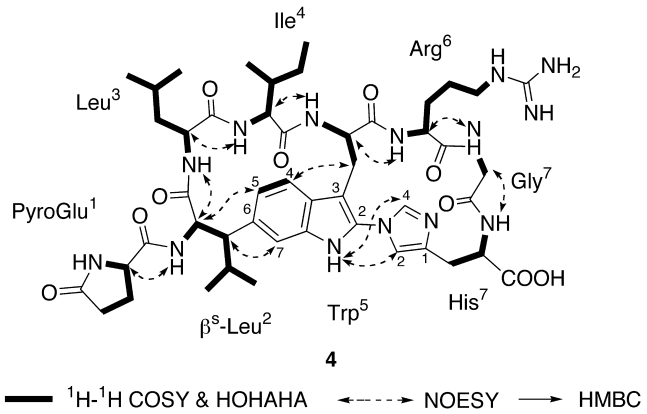

Figure 3. Selected 2D NMR correlations for celogentin G (**4**).

while those of **6** showed the presence of 1 mol each of Glu, Leu, Ile, and His, and 2 mol of Arg. ^1H and ^{13}C NMR data (Tables 1 and 2, respectively) and 2D NMR correlations for **5** and **6** were almost same as those of celogentin G (**4**) except for the presence of additional Asp^9 and Arg^9 residues for **5** and **6**, respectively. The absolute configuration of each amino acid in **5** and **6** was assigned as all L-configurations by chiral HPLC analysis of the hydrolysates of **5** and **6**, respectively. Thus, the structures of celogentins H and J were elucidated to be **5** and **6**, respectively.

1.1. Inhibition of tubulin polymerization

It is known that antimitotic peptides such as ustiloxin A,[6] arenastatin A,[7] phomopsin A,[8] and dolastatin 10[9] bind to vinca alkaloid binding site. In the previous study, celogentins A–C (**7**–**9**) and moroidin (**10**) have been found to inhibit the polymerization of tubulin.[4] In this study such inhibitory activity was observed for celogentins D–H (**1**–**5**) and J (**6**) (Table 3). Inhibitory effects of celogentins E (**2**) and C (**9**) to tubulin polymerization are shown in Figures 4 and 5, in which tubulin polymerization was inhibited in a concentration-dependent manner.

The unique $β^s$-Leu-Trp-His moiety as a common structural element may be important for inhibition of tubulin polymerization. Celogentin C (**9**: IC_{50} 0.8 μM) with a Pro residue in the right hand ring showed 30 times more potent than celogentins A (**7**: IC_{50} 20 μM) and D (**1**: IC_{50} 20 μM), and moroidin (**10**: IC_{50} 3.0 μM), and celogentins E (**2**: IC_{50} 2.5 μM) and F (**3**: IC_{50} 3.0 μM) with a Gly residue in the right hand ring showed 10 times more potent than **1** and **7**.

Table 3. Inhibitory effects of celogentins A–C (**7**–**9**), D–H (**1**–**5**), J (**6**), moroidin (**10**), and vinblastine to the polymerization of tubulin

Compounds	IC_{50} (μM)	Compounds	IC_{50} (μM)
Celogentin A (**7**)	20	Moroidin (**10**)	3.0
Celogentin B (**8**)	30	Hydrolysate **11**	20
Celogentin C (**9**)	0.8	Hydrolysate **12**	80
Celogentin D (**1**)	20	Hydrolysate **13**	>100
Celogentin E (**2**)	2.5	Hydrolysate **14**	>100
Celogentin F (**3**)	3.0	Vinblastine	3.0
Celogentin G (**4**)	4.0		
Celogentin H (**5**)	2.0		
Celogentin J (**6**)	3.0		

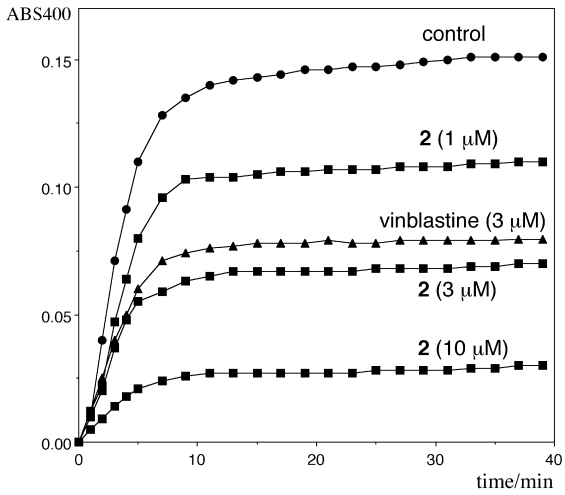

Figure 4. Inhibitory effects of celogentin E (**2**) and vinblastine to the polymerization of tubulin protein. Various concentrations of **2** were mixed with tubulin protein (1.0 mg/mL) at 0°C and incubated at 37°C.

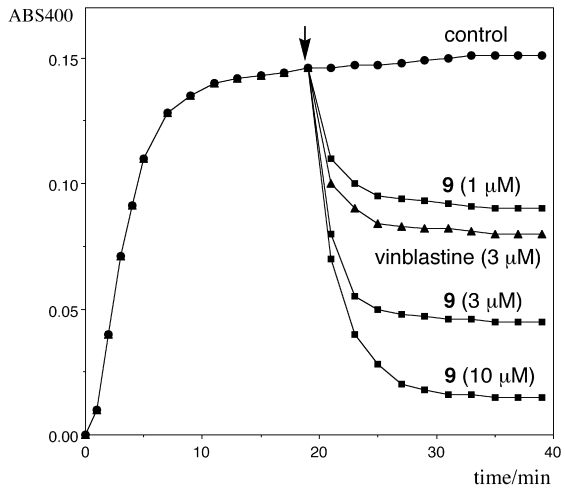

Figure 5. Effects of celogentin C (**9**) and vinblastine to the depolymerization of microtubule protein. Tubulin proteins (1.0 mg/mL) were incubated at 37°C. Various concentrations of **9** were added after 20 min incubation.

The potency of celogentins G (**4**: IC_{50} 4.0 μM), H (**5**: IC_{50} 2.0 μM), and J (**6**: IC_{50} 3.0 μM) with a Ile^4 residue was comparable to that of celogentins E (**2**) and F (**3**) with a Val^4 residue. The addition of a Lys^9 residue to celogentin B (**8**) seems not to influence severely the inhibitory activity.

On the other hand, some derivatives of moroidin (**10**) such as the Glu^1 derivative (**11**), the Glu^1 derivative with bond cleavage between the Gly^7 and His^8 residues (**12**), the Glu^1 derivative with bond cleavage between the Arg^6 and Gly^7 residues (**13**), and the derivative without the $PyroGlu^1$ residue (**14**), the last of which was prepared by treatment of moroidin (**10**) with 2N HCl, were found to be less potent (IC_{50}, 20 μM for **11**; 80 μM for **12**; >100 μM for **13**; >100 μM for **14**, respectively) than moroidin (**10**) itself, indicating that the presence of the $PyroGlu^1$ residue is important for the activity.

These bicyclic peptides are revealed to bind directly to tubulin proteins, since celogentin C (**9**) and moroidin (**10**) inhibited polymerization of tubulin proteins, which were obtained by remove of microtuble-associated proteins (MAPs) from microtubule proteins through phosphocellulose column chromatography.[12]

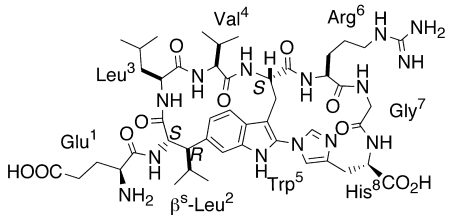

11

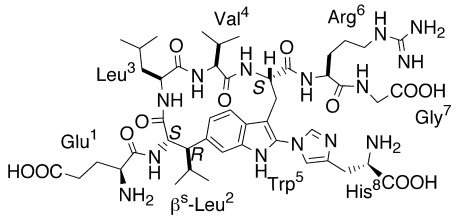

12

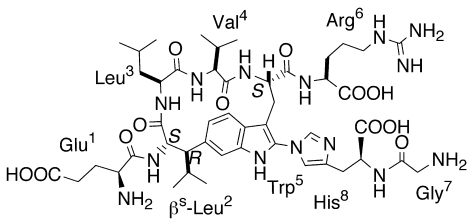

13

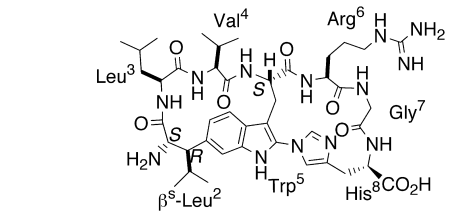

14

2. Experimental

2.1. General methods

^1H spectra were recorded in DMSO-d_6 on a 600 MHz spectrometers (Bruker AMX600) using 2.5 mm micro cells (Shigemi Co. Ltd.) at 300–330 K, while ^{13}C NMR spectra were measured on a 150 MHz spectrometer. The NMR samples of celogentins D–H and J (**1**–**6**) were prepared by dissolving 2.0 mg in 30 μL of DMSO-d_6 and chemical shifts were reported using residual DMSO-d_6 (δ_H 2.50 and δ_C 39.5) as internal standards. Standard pulse sequences were employed for the 2D NMR experiments. COSY, HOHAHA, and NOESY spectra were measured with spectral widths of both dimensions of 4800 Hz, and 32 scans with two dummy scans were accumulated into 1 K data points for each of 256 t_1 increments. NOESY and HOHAHA spectra in the phase sensitive mode were measured with a mixing time of 800 and 30 ms, respectively. For HMQC spectra in the phase sensitive

mode and HMBC spectra, a total of 256 increments of 1 K data points were collected. For HMBC spectra with *Z*-axis PFG, a 50 ms delay time was used for long-range C–H coupling. Zero-filling to 1 K for F_1 and multiplication with squared cosine-bell windows shifted in both dimensions were performed prior to 2D Fourier transformation. FABMS was measured on a JEOL JMS-HX110 by using glycerol as matrix.

2.2. Material

The seeds of *Celosia argentea* were purchased from Uchida Wakannyaku Co. in 1996. The botanical identification was made by Mr N. Yoshida, Health Sciences University of Hokkaido. A voucher specimen has been deposited in the herbarium of Hokkaido University.

2.3. Extraction and isolation

The seeds (13.5 kg) of *C. argentea* were crushed and extracted with MeOH (18 L×3), and the MeOH extract was in turn partitioned with hexane, EtOAc, and *n*-BuOH. The *n*-BuOH-soluble materials were subjected to a Diaion HP-20 column (MeOH/H_2O, 0:1→1:0), in which a fraction eluted with 60–100% MeOH was purified by an amino silica gel column ($CHCl_3$/MeOH/H_2O, 7:3:0.5→6:4:1) followed by C_{18} HPLC (CH_3CN/0.1% CF_3CO_2H, 25:75) to afford celogentins D (**1**, 0.00004% yield), E (**2**, 0.0008%), F (**3**, 0.003%), G (**4**, 0.0007%), H (**5**, 0.0004%), and J (**6**, 0.0003%), as colorless solids together with celogentins A–C (**7**–**9**) and moroidin (**10**).[5]

2.3.1. Celogentin D (1). Colorless solid; $[\alpha]_D^{24}=-33°$ (*c* 0.4, 50% MeOH); UV (MeOH) λ_{max} (log ε) 283 (3.8) and 226 (4.3) nm; IR (KBr) ν_{max} 3400, 2960, 1660, and 1545 cm^{-1}; ^1H and ^{13}C NMR (Tables 1 and 2); FABMS *m/z* 1195 $(M+H)^+$; HRFABMS *m/z* 1195.6480 (M+H; calcd for $C_{57}H_{83}N_{18}O_{11}$, 1195.6490).

2.3.2. Celogentin E (2). Colorless solid; $[\alpha]_D^{22}=-39°$ (*c* 0.5, 50% MeOH); UV (MeOH) λ_{max} (log ε) 282 (3.6) and 225 (4.2) nm; IR (KBr) ν_{max} 3390, 2930, 1660, and 1380 cm^{-1}; ^1H and ^{13}C NMR (Tables 1 and 2); FABMS *m/z* 1101 $(M)^+$; HRFABMS *m/z* 1101.5360 (M; calcd for $C_{51}H_{71}N_{15}O_{13}$, 1101.5356).

2.3.3. Celogentin F (3). Colorless solid; $[\alpha]_D^{22}=-31°$ (*c* 0.5, 50% MeOH); UV (MeOH) λ_{max} (log ε) 282 (3.6) and 225 (4.2) nm; IR (KBr) ν_{max} 3390, 2930, 1660, and 1380 cm^{-1}; ^1H and ^{13}C NMR (Tables 1 and 2); FABMS *m/z* 1143 $(M+H)^+$; HRFABMS *m/z* 1143.6180 (M+H; calcd for $C_{53}H_{79}N_{18}O_{11}$, 1143.6176).

2.3.4. Celogentin G (4). Colorless solid; $[\alpha]_D^{22}=-47°$ (*c* 1.0, 50% MeOH); UV (MeOH) λ_{max} (log ε) 283 (3.7) and 226 (4.2) nm; IR (KBr) ν_{max} 3280, 2960, 1660, 1530, and 1200 cm^{-1}; ^1H and ^{13}C NMR (Tables 1 and 2); FABMS *m/z* 1001 $(M+H)^+$; HRFABMS *m/z* 1001.5340 (M+H; calcd for $C_{48}H_{69}N_{14}O_{10}$, 1001.5322).

2.3.5. Celogentin H (5). Colorless solid; $[\alpha]_D^{22}=-40°$ (*c* 0.5, 50% MeOH); UV (MeOH) λ_{max} (log ε) 282 (3.6) and 225 (4.2) nm; IR (KBr) ν_{max} 3390, 2930, 1660, and 1380 cm^{-1}; ^1H and ^{13}C NMR (Tables 1 and 2); FABMS *m/z* 1115 $(M)^+$; HRFABMS *m/z* 1115.5570 (M; calcd for $C_{52}H_{73}N_{15}O_{13}$, 1115.5512).

2.3.6. Celogentin J (6). Colorless solid; $[\alpha]_D^{22}=-38°$ (*c* 0.4, 50% MeOH); UV (MeOH) λ_{max} (log ε) 282 (3.6) and 225 (4.2) nm; IR (KBr) ν_{max} 3390, 2930, 1660, and 1380 cm^{-1}; ^1H and ^{13}C NMR (Tables 1 and 2); FABMS *m/z* 1157 $(M+H)^+$; HRFABMS *m/z* 1157.6340 (M+H; calcd for $C_{54}H_{81}N_{18}O_{11}$, 1157.6332).

2.4. Amino acid analysis of 1–6

Each solution of **1**–**6** (0.1 mg each) in 6N HCl was heated at 110°C for 24 h in a sealed tube. After cooling, each solution was concentrated to dryness. The hydrolysates were dissolved in 0.02N HCl and subjected to amino acid analyzer.

2.5. Absolute configurations of amino acids

Each solution of **1**–**6** (each 0.1 mg) in 6N HCl (0.2 mL) was heated at 110° for 24 h. The solution was concentrated to dryness. The residue was dissolved in H_2O (50 μL) and chiral HPLC analyses were carried out using a SUMICHIRAL OA-5000 column (Sumitomo Chemical Industry; 150 mm; 25°C, detection at 254 nm). Retention times (min) of authentic amino acids were as follows: L-Glu (19.2), D-Glu (24.2), L-Val (6.1), D-Val (9.0), L-Arg (2.2), D-Arg (2.4), L-His (9.4), D-His (7.8), L-Asp (12.9), D-Asp (17.0), L-Leu (13.6), D-Leu (20.2), L-Ile (15.5), and D-Ile (22.1) [eluent: MeOH/H_2O (15:85) containing 2.0 mM $CuSO_4$, flow rate 1.0 mL/min]; L-Lys (12.0) and D-Lys (13.6) [eluent: H_2O containing 1.0 mM $CuSO_4$, flow rate 0.2 mL/min]; Retention times of the hydrolysates of **1**–**6** were as follows: **1**, L-Glu (19.1), L-Val (6.1), L-Arg (2.2), L-His (9.4), L-Leu (13.6), and L-Lys (12.0); **2**, L-Glu (19.1), L-Val (6.1), L-Arg (2.2), L-His (9.4), L-Asp (12.9), and L-Leu (13.6); **3**, L-Glu (19.1), L-Val (6.1), L-Arg (2.2), L-His (9.4), and L-Leu (13.6); **4**, L-Glu (19.1), L-Ile (15.5), L-Leu (13.6), L-Arg (2.2), and L-His (9.4); **5**, L-Glu (19.1), L-Ile (15.5), L-Leu (13.6), L-Arg (2.2), L-His (9.4), and L-Asp (12.9); **6**, L-Glu (19.1), L-Ile (15.5), L-Leu (13.6), L-Arg (2.2), and L-His (9.4).

2.6. Absolute configuration of Trp

Each celogentins D–H, and J (**1**–**6**, each 0.1 mg) in AcOH (0.2 mL) was treated with ozone at −78°C for 1 min. After removal of excess ozone by a stream of nitrogen, the mixture was treated with 30% H_2O_2 (200 μL) at room temperature for 3 h. The reaction mixture was concentrated and was hydrolyzed with 6N HCl (100 mL) at 110°C for 6 h. The hydrolysate was subjected to chiral HPLC analyses [SUMICHIRAL OA-5000, 4×150 mm; 40°C, flow rate, 1.0 mL/min; eluent; MeOH/H_2O (15:85) containing 2.0 mM $CuSO_4$]. The retention times of authentic L- and D-Asp were found to be 12.9 and 17.0 min, respectively. The retention time of Asp in the degradation products of **1**–**6** was found to be 12.9 min (L-Asp).

2.6.1. Partial hydrolysis of moroidin (10). A solution of moroidin (**10**, 10 mg) in 2N HCl was heated at 70°C for 2 h

in a sealed tube. After cooling, the solution was concentrated to dryness. The hydrolysate was subjected to C_{18} HPLC (Mightysil RP-18, 5 μm, Kanto Chemical Co., Inc., 10×250 mm; eluent, 20% CH_3CN/0.1% TFA; flow rate, 2 mL/min; UV detection at 205 nm) to afford hydrolysates **11** (1.2 mg), **12** (1.1 mg), **13** (1.0 mg), and **14** (0.9 mg). Hydrolysate **11**: ^{1}H NMR (600 MHz in DMSO-d_6, 320 K) δ 0.69 and 0.76 (each 3H, d, 6.5, Leu^3-Hδ), 0.76 and 0.79 (each 3H, d, 7.5, Val^4-Hγ), 0.76 and 0.85 (each 3H, d, 7.2, β^S-Leu^2-Hδ), 1.20 and 1.40 (each 1H, m, Leu^3-Hβ), 1.35 (each 2H, m, Leu^3-Hγ), 1.52 (2H, m, Arg^6-Hγ), 1.63 and 1.73 (each 1H, m, Arg^6-Hβ), 1.88 and 2.27 (each 1H, m, Glu^1-Hβ), 1.88 (1H, m, Val^4-Hβ), 2.16 (2H, m, Glu^1-Hγ), 2.17 (1H, m, β^S-Leu^2-Hγ), 2.64 (1H, m, Trp^5-Hβ), 2.87 and 3.12 (each 1H, m, His^8-Hβ), 3.01 (1H, dd, 3.3, 11.9, β^S-Leu^2-Hβ), 3.11 (2H, m, Arg^6-Hδ), 3.34 (1H, m, Trp^5-Hβ), 3.64 and 3.70 (each 1H, m, Gly^7-Hα), 3.74 (1H, m, Val^4-Hα), 4.01 (1H, t, 10.9, Leu^3-Hα), 3.86 (1H, m, Glu^1-Hα), 4.18 (1H, q, 7.0, Arg^6-Hα), 4.71 (1H, t, 10.4, His^8-Hα), 4.86 (1H, t, 10.4, β^S-Leu^2-Hα), 5.41 (1H, q, 8.6, Trp^5-Hα), 6.87 (1H, s, Trp^5-H7), 6.90 (1H, d, 8.0, Val^4-NH), 7.00 (1H, d, 8.3, Trp^5-H5), 7.34 (1H, m, His^8-H2), 7.51 (1H, d, 8.6, Trp^5-H4), 7.54 (1H, m, Gly^7-NH), 7.73 (1H, m, Arg^6-Hε), 7.81 (1H, d, 8.0, Trp^5-NH), 7.92 (1H, br s, His^8-H4), 8.31 (1H, s, Glu^1-NH), 8.44 (1H, d, 9.3, Leu^3-NH), 8.54 (1H, d, 7.7, His^8-NH), 8.62 (1H, d, 6.2, Arg^6-NH), 8.98 (1H, d, 8.3, β^S-Leu^2-NH), 11.52 (1H, s, Trp^5-NH1); FABMS *m/z* 1005 $(M+H)^+$; HRFABMS *m/z* 1005.5300 (M+H; calcd for $C_{47}H_{69}N_{14}O_{11}$, 1005.5270). Hydrolysate **12**: ^{1}H NMR (600 MHz in DMSO-d_6, 320 K) δ 0.69 and 0.77 (each 3H, d, 6.5, Leu^3-Hδ), 0.75 and 0.85 (each 3H, m, Val^4-Hγ), 0.74 and 0.84 (each 3H, d, 6.9, β^S-Leu^2-Hδ), 1.24 and 1.42 (each 1H, m, Leu^3-Hβ), 1.33 (1H, m, Leu^3-Hγ), 1.54 (2H, m, Arg^6-Hγ), 1.56 and 1.59 (each 1H, m, Arg^6-Hβ), 1.85 (1H, m, Val^4-Hβ), 1.89 and 2.06 (each 1H, m, Glu^1-Hβ), (1H, m, β^S-Leu^2-Hγ), 1.95 (2H, m, Glu^1-Hγ), 2.92 and 3.34 (each 1H, m, Trp^5-Hβ), 3.01 (1H, m, β^S-Leu^2-Hβ), 3.11 (2H, m, Arg^6-Hδ), 2.93, 3.03 (each 1H, m, His^8-Hβ), 3.85, 4.01 (each 1H, m, Gly^7-Hα), 3.72 (1H, m, Val^4-Hα), 3.85 (1H, m, Glu^1-Hα), 4.00 (1H, m, Leu^3-Hα), 4.55 (1H, m, His^8-Hα), 3.85 (1H, m, Arg^6-Hα), 4.83 (1H, m, β^S-Leu^2-Hα), 5.39 (1H, m, Trp^5-Hα), 6.83 (1H, s, Trp^5-H7), 7.11 (1H, m, Val^4-NH), 6.97 (1H, d, 7.8, Trp^5-H5), 7.51 (1H, m, Trp^5-H4), 7.75 (1H, m, Arg^6-Hε), 8.25 (1H, br s, Gly^7-NH), 8.39 (1H, m, Leu^3-NH), 8.23 (1H, m, Trp^5-NH), 8.73 (1H, m, Arg^6-NH), 8.97 (1H, d, 7.0, β^S-Leu^2-NH), 11.49 (1H, s, Trp^5-NH1); FABMS *m/z* 1023 $(M+H)^+$; HRFABMS *m/z* 1023.5380 (M+H; calcd for $C_{47}H_{71}N_{14}O_{12}$, 1023.5375). Hydrolysate **13**: ^{1}H NMR (600 MHz in DMSO-d_6, 320 K) δ 0.66 and 0.76 (each 3H, d, 6.2, Leu^3-Hδ), 0.67 and 0.75 (each 3H, d, 6.6, Val^4-Hγ), 0.75 and 0.82 (each 3H, d, 7.0, β^S-Leu^2-Hδ), 1.17 and 1.43 (each 1H, m, Leu^3-Hβ), 1.36 (each 2H, m, Leu^3-Hγ), 1.52 (2H, m, Arg^6-Hγ), 1.61 and 1.67 (each 1H, m, Arg^6-Hβ), 1.73 (1H, m, Val^4-Hβ), 1.88 and 2.26 (each 1H, m, Glu^1-Hβ), 2.15 (1H, m, β^S-Leu^2-Hγ), 2.16 (2H, m, Glu^1-Hγ), 2.62 and 3.32 (each 1H, m, Trp^5-Hβ), 3.04 (1H, m, β^S-Leu^2-Hβ), 3.14 (2H, m, Arg^6-Hδ), 3.16 (2H, m, His^8-Hβ), 3.32 (2H, m, Gly^7-Hα), 3.57 (1H, m, Val^4-Hα), 3.84 (1H, m, Glu^1-Hα), 3.94 (1H, m, Leu^3-Hα), 4.10 (1H, m, His^8-Hα), 4.40 (1H, m, Arg^6-Hα), 4.86 (1H, m, β^S-Leu^2-Hα), 5.69 (1H, m, Trp^5-Hα), 6.83 (1H, s, Trp^5-H7), 6.96 (1H, m, Val^4-NH), 6.96 (1H, d, 7.8, Trp^5-H5), 7.64 (1H, m, Trp^5-H4), 7.88 (1H, m, Arg^6-Hε), 8.31 (1H, br s, Gly^7-NH), 8.41 (1H, m, Leu^3-NH), 8.58 (1H, m, Trp^5-NH), 8.58 (1H, m, Arg^6-NH), 8.96 (1H, d, 7.0, β^S-Leu^2-NH), 11.73 (1H, s, Trp^5-NH1); FABMS *m/z* 1023 $(M+H)^+$; HRFABMS *m/z* 1023.5380 (M+H; calcd for $C_{47}H_{71}N_{14}O_{12}$, 1023.5376). Hydrolysate **14**: ^{1}H NMR (600 MHz in DMSO-d_6, 320 K) δ 0.72 and 0.86 (each 3H, d, 6.9, β^S-Leu^1-Hδ), 0.75 and 0.83 (each 3H, d, 6.9, Leu^2-Hδ), 0.77 (6H, d, 6.7, Val^3-Hγ), 1.24 and 1.45 (each 1H, m, Leu^2-Hβ), 1.52 (2H, m, Arg^5-Hγ), 1.57 (each 2H, m, Leu^2-Hγ), 1.67 and 1.69 (each 1H, m, Arg^5-Hβ), 2.21 (1H, m, β^S-Leu^1-Hγ), 2.63 and 3.34 (each 1H, Trp^4-Hβ), 2.84 and 3.09 (each 1H, m, His^7-Hβ), 2.98 (1H, m, β^S-Leu^1-Hβ), 3.12 (2H, m, Arg^5-Hδ), 3.64 and 3.67 (each 1H, m, Gly^5-Hα), 3.70 (1H, m, Val^3-Hα), 4.01 (1H, m, β^S-Leu^1-Hα), 4.02 (1H, m, Leu^3-Hα), 4.19 (1H, m, Arg^5-Hα), 4.64 (1H, m, His^7-Hα), 5.37 (1H, m, Trp^5-Hα), 6.76 (1H, m, Val^3-NH), 6.83 (1H, s, Trp^4-H7), 6.89 (1H, d, 8.8, Trp^5-H5), 7.46 (1H, d, 8.9, Trp^5-H4), 7.61 (1H, m, Gly^6-NH), 7.69 (1H, m, Arg^5-Hε), 7.84 (1H, m, Trp^4-NH), 8.43 (1H, m, His^7-NH), 8.60 (1H, m, Leu^2-NH), 8.61 (1H, m, Arg^5-NH), 11.49 (1H, s, Trp^4-NH1); FABMS *m/z* 875 $(M+H)^+$; HRFABMS *m/z* 876.4837 (M+H; calcd for $C_{42}H_{62}N_{13}O_8$, 876.4845).

2.7. Preparation of microtubule protein

Microtubule protein was prepared from porcine brain as described previously.[10] The protein concentrations were determined by the method of Lowry et al.[11] using bovine serum albumin as a standard. Microtubule assembly assays were carried out in MES buffer containing 100 mM 2-*N*-morpholino ethanesulfonic acid (MES), 1 mM ethylene-bis(oxyethylenenitrilo)-tetraacetic acid (EGTA), 0.5 mM $MgCl_2$, 1 mM 2-mercaptoethanol, and 1 mM guanosine 5″-triphosphate trisodium salt (GTP) (pH 6.5).

2.8. Preparation of tubulin protein

Tubulin was purified from microtubule protein by phosphocellulose column chromatography.[12] Protein concentration were determined by the method of Lowry et al.[11] using bovine serum albumin as a standard. Purity was assayed by polyacrylamide gel electrophoresis (PAGE).[13]

2.9. Microtubule assembly assay

Microtubule assembly was monitored spectroscopically by using a spectrophotometer equipped with a thermostatically regulated liquid circulator. The temperature was held at 37°C and changes in turbidity were monitored at 400 nm. For the drug-protein studies, 10 μM of drug dissolved in DMSO concentration was less than 1%. The turbidity changes were monitored throughout the incubation time.

Acknowledgements

The authors thank Mrs S. Oka and Miss M. Kiuchi, Center for Instrumental Analysis, Hokkaido University, for measurements of FABMS. This work was partly supported by a Grant-in-Aid from the Ministry of Education, Science, Sports, and Culture of Japan, and grants from the Hokkaido Foundation for the Promotion of Scientific and Industrial

Technology and Shorai Foundation for Science and Technology.

References

1. For reviews of the antimitotic agents, see: (a) Iwasaki, S. *Med. Res. Rev.* **1993**, *13*, 183–198. (b) Hamel, E. *Med. Res. Rev.* **1996**, *16*, 207–231.
2. (a) Haar, E.; Kowalski, R. J.; Hamel, E.; Lin, C. M.; Longley, R. E.; Gunasekera, S. P.; Rosenkranz, H. S.; Day, B. W. *Biochemistry* **1996**, *35*, 243–250. (b) Kowalski, R. J.; Giannakakou, P.; Hamel, E. *J. Biol. Chem.* **1997**, *272*, 2534–2541.
3. Kobayashi, J.; Suzuki, H.; Shimbo, K.; Takeya, K.; Morita, H. *J. Org. Chem.* **2001**, *66*, 6626–6633.
4. Morita, H.; Shimbo, T.; Shigemori, H.; Kobayashi, J. *Bioorg. Med. Chem. Lett.* **2000**, *10*, 469–471.
5. (a) Leung, T.-W. C.; Williams, D. H.; Barna, J. C. J.; Foti, S. *Tetrahedron* **1986**, *42*, 3333–3348. (b) Leung, T.; W, C.; Williams, D. H.; Barna, J. C. J.; Foti, S. *J. Org. Chem.* **1989**, *54*, 1901–1904. (c) Kahn, S. D.; Booth, P. M.; Waltho, J. P.; Williams, D. H. *J. Org. Chem.* **2000**, *65*, 8406.
6. Li, Y.; Koiso, Y.; Hashimoto, Y.; Iwasaki, S. *Biochem. Pharmacol.* **1995**, *49*, 1367–1372.
7. (a) Koiso, Y.; Morita, K.; Kobayashi, M.; Wang, W.; Ohyabu, N.; Iwasaki, S. *Chem. Bio. Interact.* **1996**, *102*, 183–191. (b) Morita, K.; Koiso, Y.; Hashimoto, Y.; Kobayashi, M.; Wang, W.; Ohyabu, N.; Iwasaki, S. *Biol. Pharm. Bull.* **1997**, *171*, 174.
8. Li, Y.; Kobayashi, H.; Tokiwa, Y. *Biochem. Pharmacol.* **1992**, *43*, 219–224.
9. Li, Y.; Kobayashi, H.; Hashimoto, Y. *Chem. Bio. Interact.* **1994**, *93*, 175–183.
10. Takahashi, M.; Iwasaki, S.; Kobayashi, H.; Okuda, S.; Murai, T.; Sato, Y.; Haraguchi-Hiraoka, T.; Nagano, H. *J. Antibiot.* **1987**, *40*, 66–72.
11. Lowry, O. H.; Rosebrough, N. J.; Farr, A. L.; Randall, R. J. *J. Biol. Chem.* **1951**, *193*, 265–275.
12. William, R. C.; Lee, J. C. *Methods Enzymol.* **1982**, *85*, 376.
13. Laemmli, U. K. *Nature* **1970**, *227*, 680–685.